Supporting Information

Vertically Aligned Nanorods Fe_2TiO_5 and Coupling of $NiMoO_4$/$CoMoO_4$ as A Hole-Transfer Cocatalyst for Enhancing Photoelectrochemical Water Oxidation Performance

Baohua Ding[a], Haiyan Li[a], Ruonan Wang[a], Bohua Dong[a,*], Lixin Cao[a,*]

[a] School of Materials Science and Engineering, Ocean University of China, 238 Songling Road, Qingdao, 266100, PR China

[*] Corresponding authors

[*] E-mail: caolixin@ouc.edu.cn (L. Cao), dongbohua@ouc.edu.cn (B. Dong).

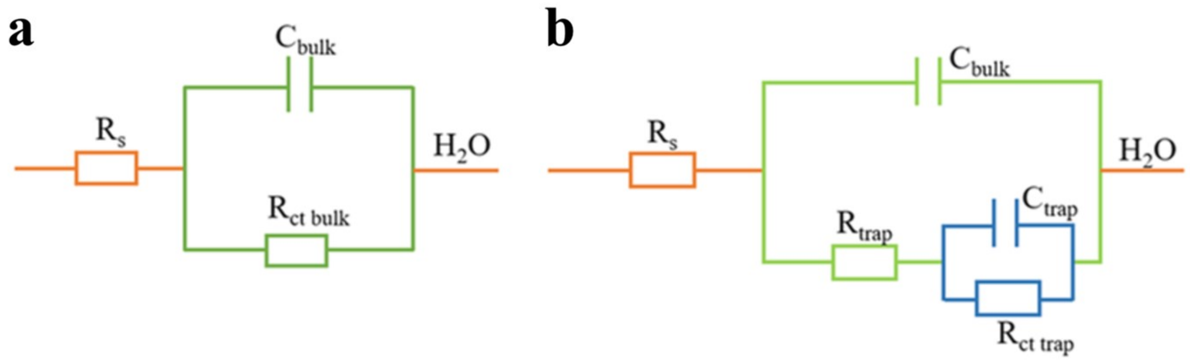

Figure S1. (a) Equivalent circuit (EC) for the charge transfer process of Fe_2TiO_5 composite photoanode under dark, R_s, resistance associated with the electric contact of the electrode, electrolyte, etc. C_{bulk}, Bulk capacitance of Fe_2TiO_5 related to charge accumulation. $R_{ct\ bulk}$, Resistance of hole transfer from Fe_2TiO_5 composite photoanode to water molecule. there is no surface states mediated process under dark. (b) Equivalent circuit (EC) for the charge transfer process of Fe_2TiO_5 composite photoanode under illumination, the Fe_2TiO_5 SEI is mediated by surface states. R_s, resistance associated with the electric contacts of the electrode, electrolyte, etc. C_{bulk}, Bulk capacitance of Fe_2TiO_5 related to charge accumulation. R_{trap}, Surface state hole trapping resistance. $R_{ct\ trap}$, Resistance of hole transfer from surface state to water molecule. C_{trap}, Surface state charge accumulation capacitance.

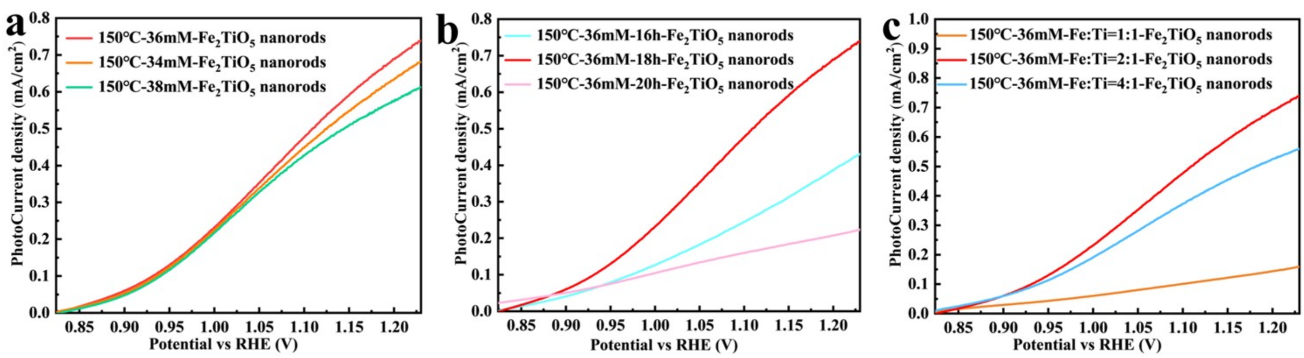

Figure S2. (a) precursor solution concentration, (b) hydrothermal time and (c) ratio of iron to titanium atoms in precursor solution optimization process shown in J-V curves. The optimization results were 36 mM,18 h,2:1, respectively.

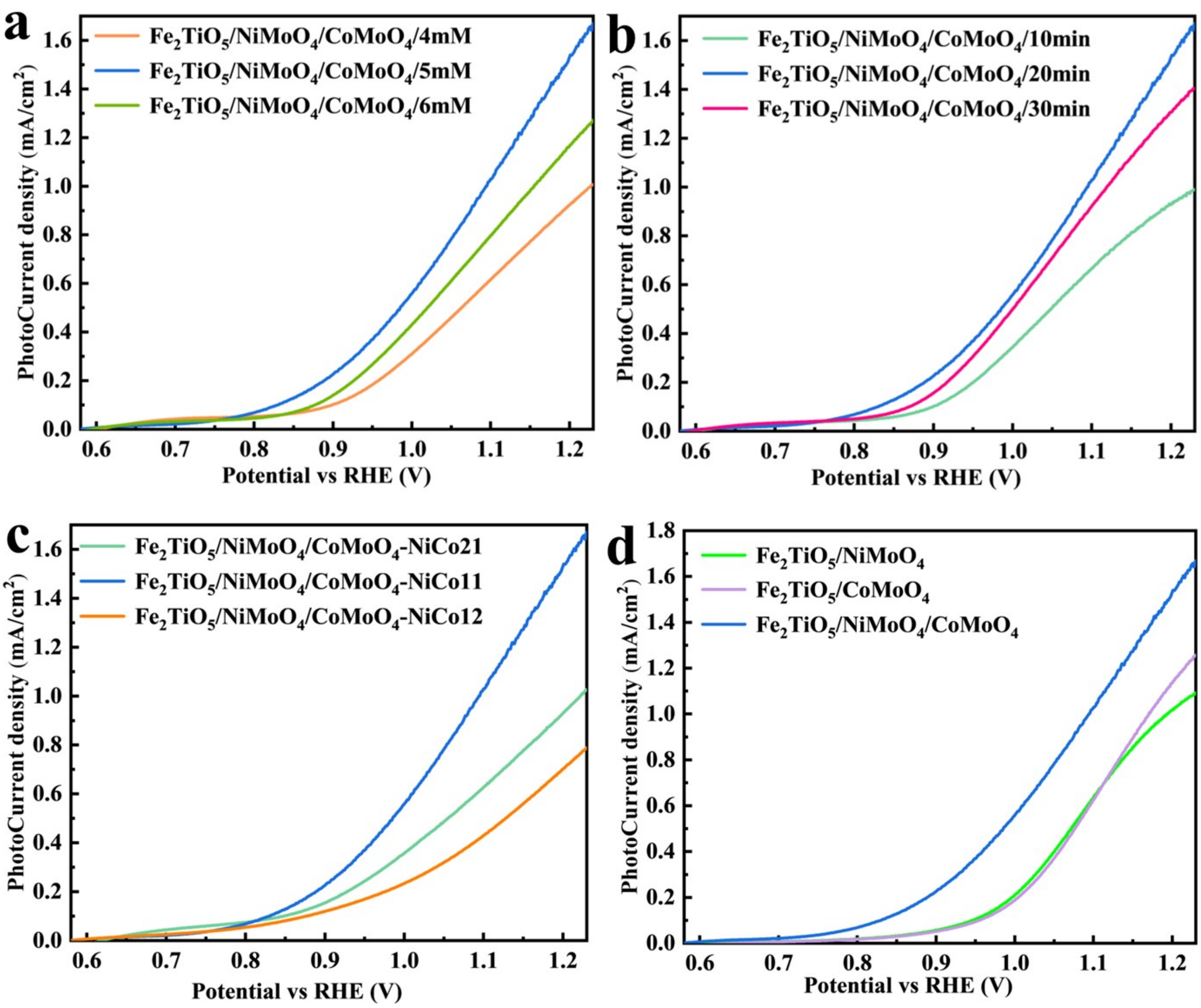

Figure S3. (a) precursor solution concentration, (b) hydrothermal time, (c) ratio of cobalt to nickel atoms in precursor solution and (d) species of cobalt and nickel atoms in precursor solutions optimization process shown in J-V curves. The optimization results were 5mM, 20min, CoNi-11, $NiMoO_4$/ $CoMoO_4$.

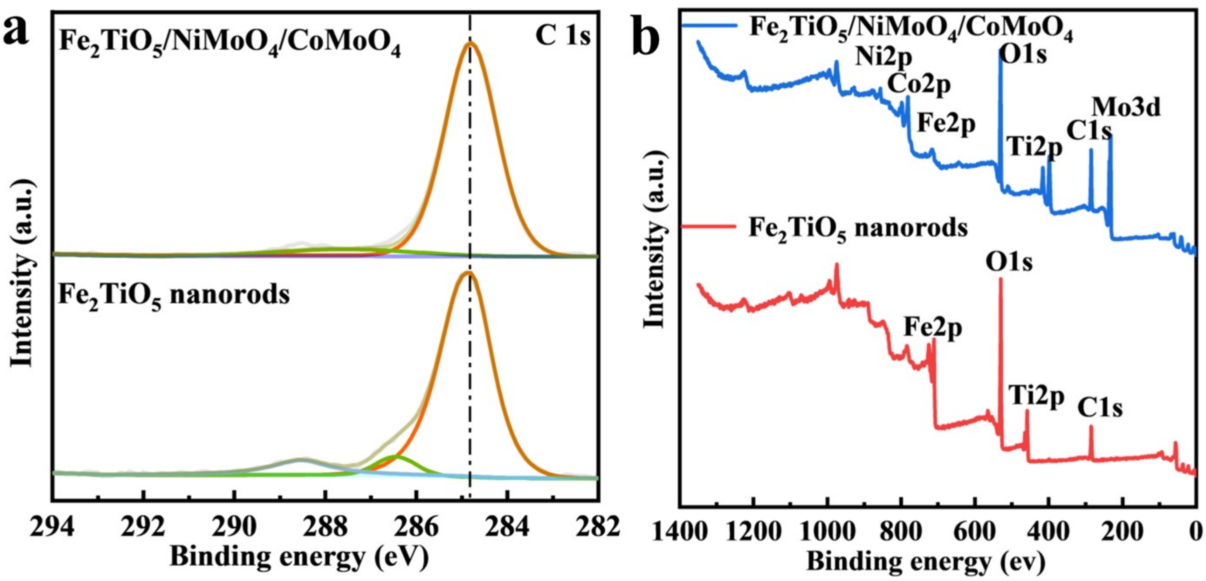

Figure S4. XPS spectrum of (a) C1s, (b) XPS survey spectrum of $Fe_2TiO_5/NiMoO_4/CoMoO_4$.

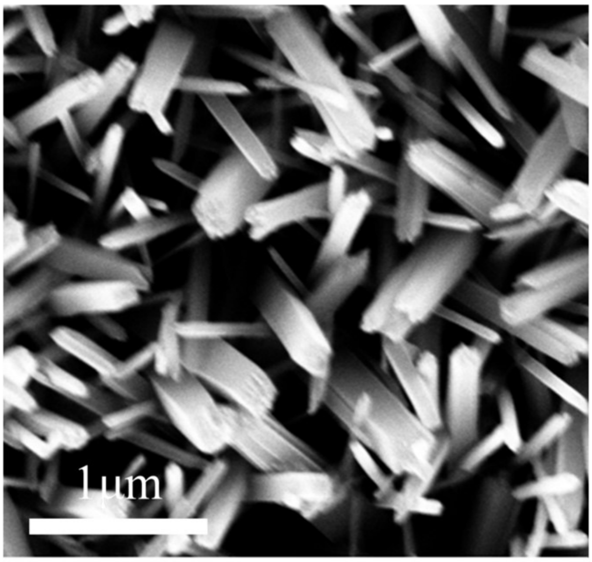

Figure S5. SEM image of TiO_2 nanorods.

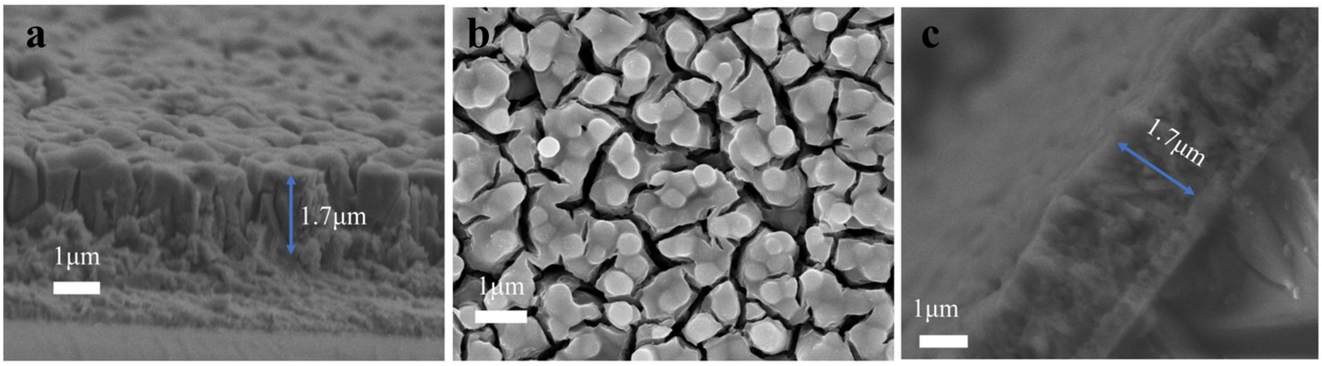

Figure S6. SEM images of (a) cross-sectional of Fe_2TiO_5 nanorods, (b) $Fe_2TiO_5/NiMoO_4/ CoMoO_4$ and (c) cross-sectional of $Fe_2TiO_5/NiMoO_4/CoMoO_4$.

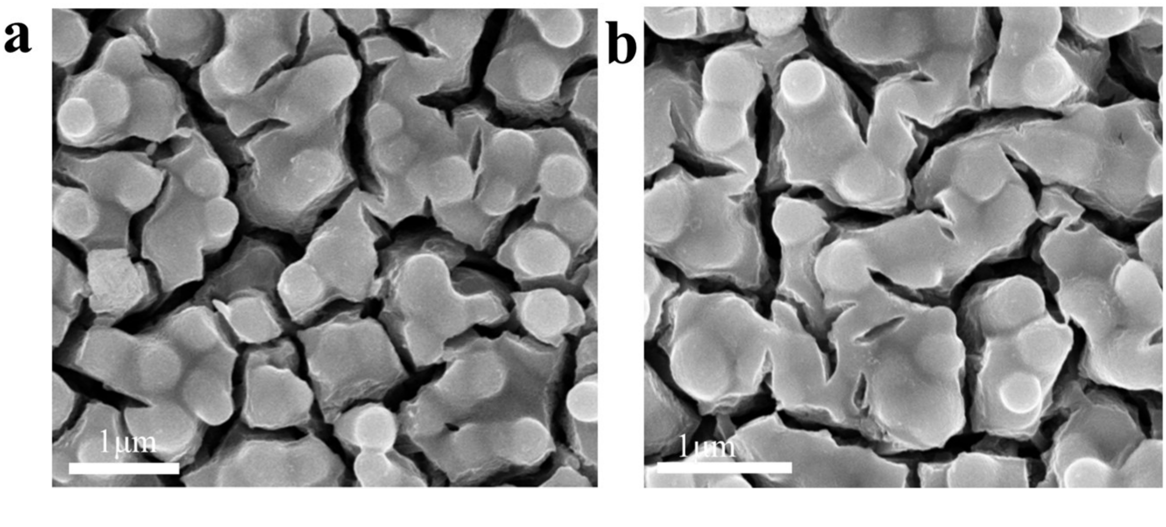

Figure S7. SEM images of $Fe_2TiO_5/NiMoO_4/CoMoO_4$ (a) before and (b) after 2 hours of stability measurement.

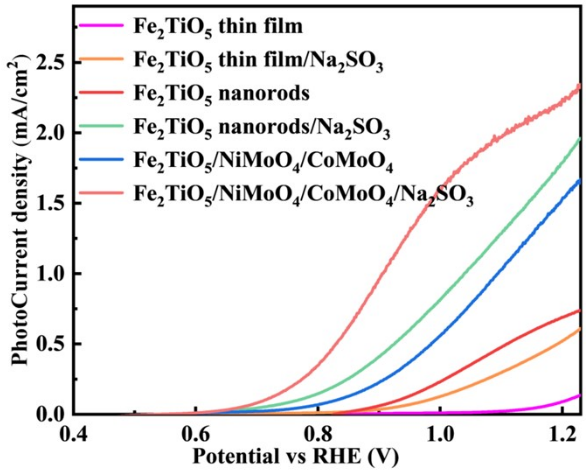

Figure S8. J–V curves of Fe_2TiO_5 thin film, Fe_2TiO_5 nanorods and $Fe_2TiO_5/NiMoO_4/CoMoO_4$ in 1.0 M KOH with and without 0.5M Na_2SO_3 under AM 1.5 G irradiation.

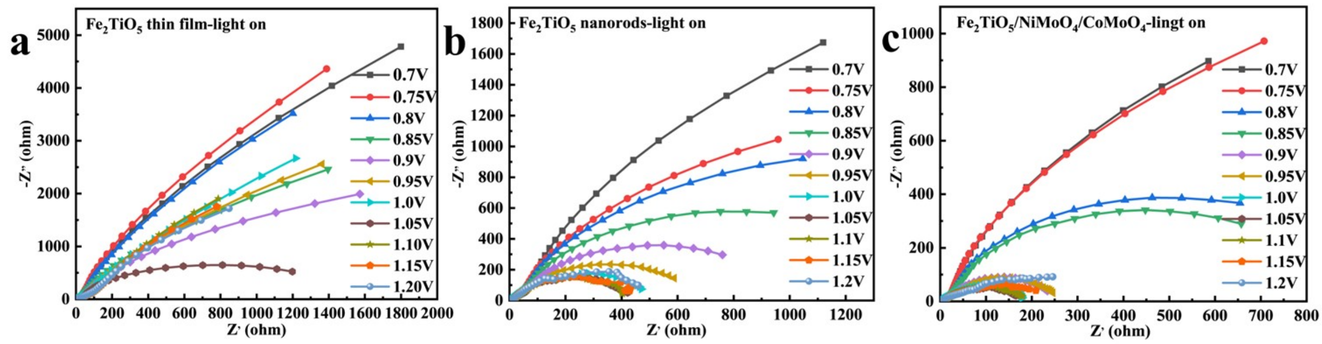

Figure S9. Nyquist plots under light illumination of (a) Fe_2TiO_5 thin film, (b) Fe_2TiO_5 nanorods and (c) $Fe_2TiO_5/NiMoO_4/CoMoO_4$ at 0.7, 0.75, 0.8, 0.85, 0.9, 0.95, 1.0, 1.05, 1.1, 1.15, 1.2 V_{RHE}.

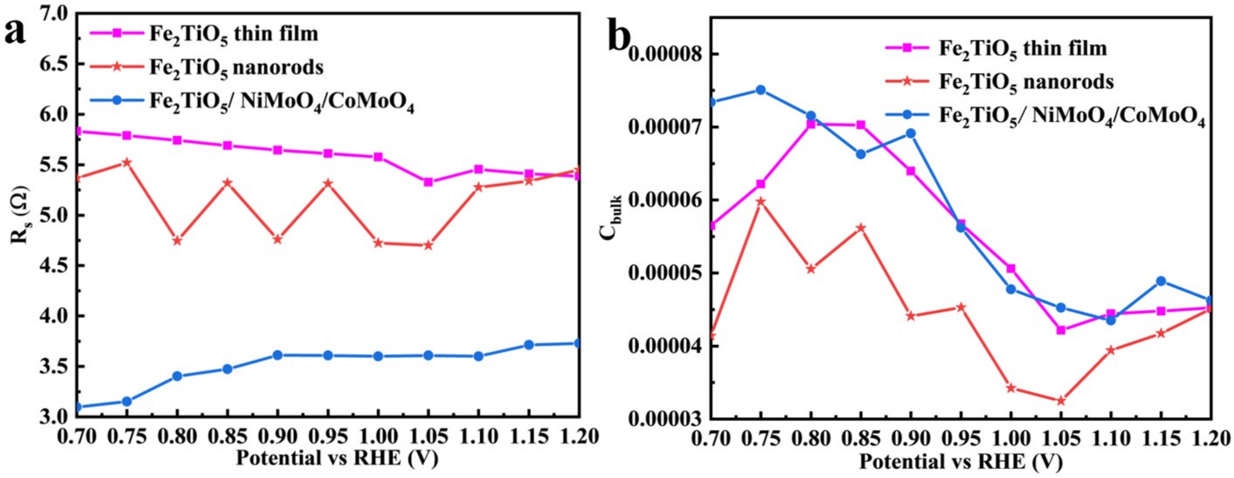

Figure S10. (a) R_s, (b) C_{bulk} fitting values from the impedance response of the Fe_2TiO_5 thin film, Fe_2TiO_5 nanorods and $Fe_2TiO_5/NiMoO_4/CoMoO_4$ under AM 1.5 G illumination.

As Figure S9. (a) shown the values of R_s follow this order: Fe_2TiO_5 thin film> Fe_2TiO_5 nanorods> $Fe_2TiO_5/NiMoO_4/CoMoO_4$.The results reflected that nanorods allowed directional electron transport to the back substrates more easily than flat films, reducing contact resistance. After loading the $NiMoO_4/CoMoO_4$, not only the backside contact resistance, but also the contact resistance between the composite photoanode and electrolyte was greatly reduced, and Rs was greatly reduced. Figure S9. (b) showed that $Fe_2TiO_5/NiMoO_4/CoMoO_4$ and Fe_2TiO_5 thin film had similar C_{bulk} values, but Fe_2TiO_5 thin film had the lowest photoelectric response. This may be the fact that all the holes of Fe_2TiO_5 thin film were concentrated in the bulk of Fe_2TiO_5 thin film, resulting in serious bulk recombination. This viewpoint had also been verified when discussing the R_{trap}, $R_{ct\ trap}$, C_{trap} and DOS.